Talanta Open 9 (2024) 100319

Contents lists available at ScienceDirect

Talanta Open

journal homepage: www.sciencedirect.com/journal/talanta-open

Dynamic cell photo-manipulation technology for the molecular and mechanical regulation analyses of collective cell migration

Kazuhiro Tatematsu [a,b], Shota Yamamoto [a], Masao Kamimura [c], Kazuo Yamaguchi [d], Jun Nakanishi [a,b,c,*]

[a] Research Center for Macromolecules and Biomaterials, National Institute for Materials Science (NIMS), 1-1 Namiki, Tsukuba, Ibaraki 305-0044, Japan
[b] Graduate School of Advanced Science and Engineering, Waseda University, 3-4-1 Okubo, Shinjuku-ku, Tokyo 169-8555, Japan
[c] Graduate School of Advanced Engineering, Tokyo University of Science, 6-3-1 Niijuku, Katsushika-ku, Tokyo 125-8585, Japan
[d] Department of Chemistry, Faculty of Science, Kanagawa University, 3-27-1 Rokukakubashi, Yokohama, Kanagawa 231-8686, Japan

ARTICLE INFO

Keywords:
Collective cell migration
Dynamic substrate
Mechanobiology
Extracellular matrix

ABSTRACT

Collective cell migration is an essential biological process. Migration behaviors of multiple cellular units depend on the mechanical and chemical properties of their scaffolds and the geometry of the cells. However, the mechanisms by which these properties synergistically regulate the collective cell characteristics remain unknown. A robust method is required to analyze collective cell migration. Therefore, in this study, we developed a new method for collective cell migration analysis using defined chemical, mechanical, and geometrical properties. Our method is based on a poly(acrylic acid) hydrogel, whose surface is functionalized with photocleavable poly(ethylene glycol) and a cell-adhesive peptide. By controlling the UV irradiation of the photoactivatable hydrogel, we created geometrically controlled cellular clusters and induced collective migration. Furthermore, chemical and mechanical cues exposed to cell clusters were manipulated depending on the surface density of the cell-adhesive peptide and crosslinking density of the hydrogel. As a proof of concept, we also demonstrated that the collective migration of epithelial cells was synergistically regulated by the chemical and mechanical properties of the scaffold. Our results suggest the new photoactivatable substrate as a promising tool for advanced molecular and mechanobiological analyses of collective cell migration.

Introduction

Collective cell migration is a key activity observed in embryonic morphogenesis, wound healing, and cancer invasion [1]. Similar to the migration of single cells, the driving force of collective migration is the actomyosin-mediated contractile force. However, collective cells express unique supercellular features, such as collective polarization into leader and follower cells, force transmission, and decision making *via* cadherin-mediated cell–cell contact [2,3]. These collective characteristics are highly dependent on the global morphology and size of the cell clusters [4]. For example, alignment of cells within cellular clusters depends on their geometry; this alignment generates mechanical stress polarization within the cellular cluster [5]. Consequently, stress polarization mechanically increases the frequency of leader cell formation [5]. In addition to endogenous cues within cell collectives derived from their own cellular geometries, exogenous cues, such as biochemical and mechanical signals from the extracellular matrix (ECM), alter the collective migration behaviors [6,7]. Various mechanical properties, such as substrate stiffness, affect the collective cell migration in response to ROCK-mediated myosin contraction [8]. Activity of the integrin β_1 receptor, which regulates cell adhesion, may be associated with the functions of leader cells [9]. These studies indicate that collective cell migration is regulated by chemical signaling. Therefore, a robust methodology is required to analyze the migration of cell collectives with defined geometries under controlled chemical and mechanical cues.

Wound healing assay is a widely used method for cell migration analysis to determine the effects of drugs or gene expression on cell migration activities [10]. However, this conventional method is not suitable for the precise analysis of collective cell migration as the endogenous and exogenous cues can be readily changed depending on the study technique and experimental conditions. Moreover, the geometry of cellular clusters cannot be controlled in this method, and there is a possibility of confounding the results due to the effects of the cellular debris generated during the cell scratching process [11]. To overcome

* Corresponding author.
E-mail address: NAKANISHI.Jun@nims.go.jp (J. Nakanishi).

https://doi.org/10.1016/j.talo.2024.100319
Received 7 December 2023; Received in revised form 17 April 2024; Accepted 20 April 2024
Available online 25 April 2024

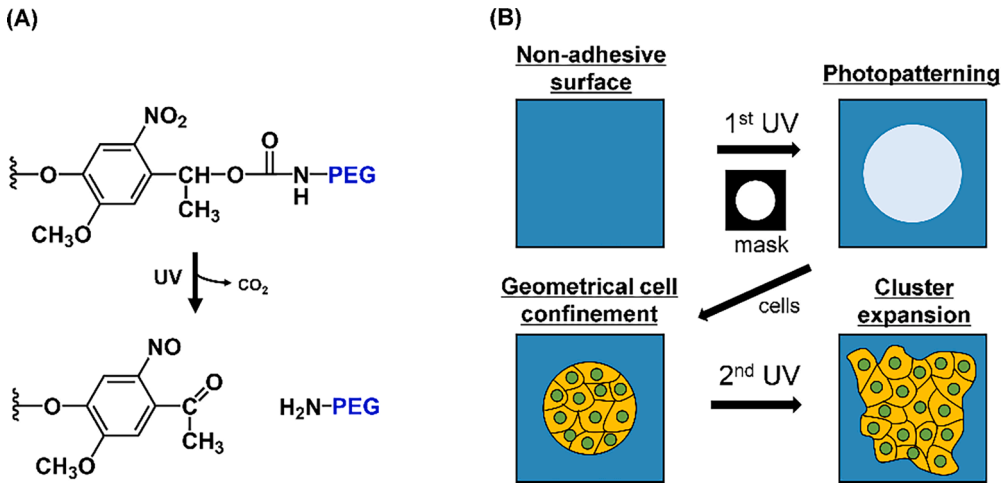

Fig. 1. Schematic illustration of the photoactivatable surface based on photocleavable poly(ethylene glycol) (PEG) that changes from non-cell-adhesive to cell-adhesive in response to UV light. (A) Essential photochemical reaction of photocleavable PEG. (B) Procedure for cell patterning and migration induction on the photoactivatable surface. Deep blue area, non-cell adhesive surface. Light blue area, cell adhesive surface.

these problems, a migration assay based on a polydimethylsiloxane (PDMS) stencil has been developed [12]. The PDMS stencil geometrically defines the cell adhesion area and induced migration by peeling off PDMS from the substrate surface. This assay can be applied to various types of biomaterials, such as tissue culture polystyrene and hydrogels, to control the chemical and mechanical cues [13,14]. However, this method requires the application of force to peel off the PDMS stencil, leading to the mechanical perturbation of cells close to the edge region. In addition, this peeling-off step increases the difficulty of observing the onset of collective cell migration immediately after stencil removal.

In recent years, several engineered biomaterial platforms that can dynamically and remotely manipulate cells have been developed to overcome these challenges [15,16]. In particular, photoresponsive platforms for collective cell migration analysis have attracted attention as dynamic biomaterials for the control of cellular behaviors in a non-invasive manner [17]. Light stimuli have high spatiotemporal resolution, even at the single-cell level [15,17]. Furthermore, light stimulation can be applied remotely to the material, facilitating real-time observation of the onset of cell population movement. Therefore, we previously developed a robust approach to make material surfaces photoactivatable using photocleavable poly(ethylene glycol) (PEG) (PCP) with a 2-nitrobenzyl group [17–24] (Fig. 1a). The material surface, which is initially non-cell-adhesive due to the presence of protein- and cell-repellent PEG, allows surface cell adhesion after the removal of PEG *via* UV irradiation (λ = 365 nm) [17–24]. Therefore, instead of creating a physical barrier in the stencil assay, we can create cell clusters with an arbitrary geometry and induced their migration *via* spatiotemporally controlled photoirradiation (Fig. 1b). This concept can also be applied to various materials because its working principle is based on interfacial photochemical reaction [24]. For example, photoactivatable hydrogels have been developed by conjugating PCP to the surface of poly(acrylamide) hydrogels to study the effects of mechanical cues on collective cell migration [21,23]. In addition, the effects of (bio)chemical cues on nanopatterned or gold substrates co-immobilized with an ECM-mimetic cyclic(Arg-Gly-Asp) (cRGD) peptide and PCP have been investigated [19,20,22]. These platforms are based on different base materials, such as elastic hydrogels and rigid glass/gold substrates. By integrating the functions of photoactivatable substrates, these platforms can accurately assess the crosstalk between the molecular and mechanical regulation mechanisms of collective cell migration.

In this study, we aimed to develop a novel photoactivatable substrate with tuned cRGD surface density and stiffness. Here, we developed a new photofunctionalization method to co-immobilize PCP and cRGD onto the surface of a poly(acrylic acid) (PAA) hydrogel. In addition, as a proof of concept, we demonstrated the photopatterning of cellular clusters corresponding to the photopattern and phototriggered collective cell migration to the hydrogel surface by controlling UV irradiation.

Experimental

Reagents and materials

Acetonitrile (CH_3CN), super dehydrated acetonitrile (dry CH_3CN), diethyl ether, methanol, dichloromethane, 1,2-ethylenediamine, hydrochloric acid, magnesium sulfate anhydrous, sodium hydroxide, *N,N,N',N'*-tetramethylethylenediamine (TEMED), acrylic acid, 1-ethyl-3-(3-dimethylaminopropyl)carbodiimide hydrochloride (EDC), penicillin–streptomycin, and Wakogel® C-300 (silica Gel) were purchased from Wako Pure Chemical Industries (Osaka, Japan). Moreover. 3-(methacryloyloxy) was purchased from TCI (Tokyo, Japan). Here, 1-(5-methoxy-2-nitro-4-prop-2- ynyloxyphenyl)ethyl *N*-succinimidyl carbonate (**1**) was synthesized as previously described [18]. Copper bromide(I) (99.999 %) (CuBr(I)), ammonium peroxodisulfate (APS), minimum essential medium (MEM), and L-glutamine were purchased from Sigma-Aldrich (St. Louis, MO, USA). α-methoxy-ω-azide-poly (ethylene glycol) (MeO-PEG-N_3; M_n = 5000) was purchased from Iris Biotech (Marktredwitz, Germany). Cyclo[Arg-Gly-Asp-D-Phe-Lys(PEG--PEG)] was purchased from Peptide Institute. Inc. (Osaka, Japan). MEM nonessential amino acids (MNEAA) and trypsin-EDTA solution were purchased from Invitrogen (Carlsbad, CA, USA). Glass coverslips (0.12–0.17 mm thick) were purchased from Matsunami (Osaka, Japan). *N,N'*-methylenebis(acrylamide) was purchased from Bio-Rad (Hercules, CA, US), and SUS304 steel balls (diameter = 0.5 mm) were obtained from Funabe Seiko (Nishinomiya, Japan). Molecular Probes™ FluoSpheres™ Amine-Modified Microspheres was purchased from Thermo fisher Scientific (Waltham, MA, US).

1-(5-Methoxy-2-nitro-4-(prop-2-yn-1-yloxy)phenyl)ethyl (2-aminoethyl) carbamate (2)

Photocleavable linker (**2**) was synthesized as described below. **1** (0.50 g, 1.28 mmol) was weighed into a separatory funnel and dissolved in 25 mL of CH_3CN. This solution was dropped onto 1,2-ethylendiamine (76.9 g, 128 mmol) over 1 h and concentrated on a rotary evaporator to remove the unreacted 1,2-ethylendiamine. Then, water (50 mL) and 2 N HCl (6 mL) were added, and the solution was extracted with dichloromethane (3 × 50 mL). Subsequently, 1 N NaOH (10 mL) was added to the water layer, and the solution was extracted with dichloromethane (3

× 50 mL). The organic layer was dried over $MgSO_4$, and the solvent was removed under reduced pressure to yield 270 mg (0.800 mmol, 62.5 %). Proton nuclear magnetic resonance (^{1}H NMR; 300 MHz, $CDCl_3$, TMS) = 1.30 (brs, 2H, NH_2), 1.59–1.61 (d, 3H, J = 6.0 Hz; CH_3), 2.57–2.59 (t, 1H, J = 3.0 Hz; CH), 2.79–2.83 (t, 2H, J = 6.0 Hz; CH_2), 3.17–3.22 (t, 2H, J = 6.0 Hz; CH_2), 4.00 (s, 3H; CH_3), 4.81–4.82 (d, 2H, J = 3.0 Hz; CH_2), 5.20 (s, 1H; NH), 6.38–6.40 (q, 1H, J = 6.0 Hz; CH), 7.04 (s, 1H; Ar H), 7.76 (s, 1H; Ar H).

Amino-terminated photocleavable poly(ethylene glycol)) (3)

Synthesized compound **3** was named PCP5k-NH_2 depending on the molecular weight of MeO-PEG5k-N_3 and synthesized as described below. MeO-PEG5k-N_3 (M_n = 5000, 600 mg 0.12 mmol), **2** (47.2 mg, 0.14 mmol), and Cu(I)Br (20.0 mg, 0.24 mmol) were weighed in a two-neck round-bottom flask and dissolved in 10 mL of dry CH_3CN. The solution was subsequently stirred at room temperature for 24 h under a nitrogen atmosphere and light shading. After concentrating the solution on a rotary evaporator, dichloromethane (5 mL) was added, and the solution was dropped into diethyl ether (50 mL) in an ice bath for 1 h to remove the unreacted photoactivatable linkers *via* reprecipitation. The precipitate was filtered off and purified *via* column chromatography (Wakogel® C-300/dichloromethane: methanol = 9:1). Finally, the recovered polymer was freeze-dried in water for 24 h to obtain **3**. The final yield of the polymer was 10 mg (0.0020 mmol, 1.7 %) as a light yellow solid. PCP5k-NH_2 was obtained at 57 % purity. (^{1}H NMR; 300 MHz, $CDCl_3$, TMS) = 1.25 (s, 2H; NH_2), 1.59–1.61 (d, 3H, J = 8.0 Hz; CH_3), 3.06 (brs, 2H; CH_2), 3.39–3.43 (m, 5H; CH_3, CH_2) 3.51–3.90 (m, 789H; CH_2), 4.05 (s, 3H; CH_3), 4.54–4.57 (brs, 2H; CH_2) 5.27–5.38 (m, 3H; NH, CH_2), 6.36–6.42 (q, 1H, J = 8.0 Hz; CH), 7.72 (s, 1H; Ar H), 7.92 (m, 1H; Ar H), 7.94 (m, 1H; N—H-N). Because of the difficulty in complete removal of unreacted MeO-PEG5k-N_3 from the final product, we used the crude mixture since the remaining MeO-PEG5k-N_3 do not affect the following surface modification reaction and can be removed from the system during the washing step.

Preparation of methacrylate-modified glass coverslips

Surfaces of glass coverslips were functionalized as previous reported [21,23]. In the surface functionalization method, glass coverslips were first cut into pieces (10 mm × 10 mm) and cleaned ultrasonically at room temperature for 5 min *via* immersion in methanol. The surfaces of the glass coverslips were then cleaned using a UV-O_3 cleaner for 1 h and immersed in a 0.4 wt% methanol solution of 3-(methacryloyloxy)propyltrimethoxysilane at room temperature for 1 h. After the reaction, the samples were washed thrice with methanol and dried under nitrogen gas at room temperature.

Preparation of stiffness-tuned PAA hydrogel substrates and characterization of their mechanical properties

PAA hydrogel substrates were prepared as follows. First, a pre-gel solution containing TEMED (150 μL), phosphate-buffered saline (PBS) buffer (400 μL), 5.6 M acrylic acid solution (300 μL), and 0.13 M *N,N'*-methylenebis(acrylamide) solution (300 or 160 μL) were prepared. These concentrations were chosen to obtain two distinct stiffness based on the recipe known in poly(acrylamide) hydrogel formations [25]. Next, the pre-gel solution was degassed using a diaphragm pump at room temperature for 1 h, and an 0.44 M APS solution (12 μL) added into the pre-gel solution. Next, a 10 μL droplet of that solution was rapidly pipetted onto the polytetrafluoroethylene (PTFE) sheet. The droplets on the PTFE sheet were immediately covered with a methacrylate-modified glass coverslip. Polymerization was completed in approximately 25 min at 80°C. Finally, the PTFE sheet was carefully peeled off, and the gel surface was washed thrice with PBS. The stiffness of the hydrogel was characterized by a gel indentation assay. This assay gives the Young's modulus of elastic hydrogels such as a poly(acrylamide) hydrogel through a simple method [26]. Briefly, a commercially available aqueous solution of fluorescent beads diluted by 10,000-fold with ultrapure water was dropped to the hydrogel surface, and then a steal ball of a given density (g/cm^3) was placed onto the surface. Then the z-position of the fluorescent beads directly under the steal ball was focused with a confocal microscope and recorded. Finaly, the steal ball was removed with ultrapure water from a pipette and the z-position of the same fluorescent beads was recorded. The elastic modulus was calculated based on the displacement of the z-position of the fluorescent beads by using the equation shown in the reference.

Photofunctionalization of the surface of PAA hydrogel substrates

A 50 μL droplet of PBS aqueous solution containing PCP5k-NH_2 (8 mg/mL) and EDC (19 mg/mL) was pipetted onto the surface of PAA hydrogel substrates and reacted at room temperature for 1 h under light-shading condition. The PEGylated surface via the photocleavable group was rinsed with PBS 3 times. Next, a 50 μL droplet of PBS aqueous solution of cRGD which was prepared appropriate concentration was pipetted onto the surface of PAA hydrogel substrates and reacted at room temperature for 24 h under light-shading condition. Using the steps described above, we co-immobilized PCP5k-NH_2 and cRGD-NH_2 onto the surfaces of the hydrogels. After shaking the substrates with immersion in PBS for 24 h, a passivated hydrogel surface was obtained, on which the cells could not adhere unless the surface was photoirradiated.

Cell culture

Madin–Darby canine kidney (MDCK) epithelial cells were obtained from the RIKEN cell bank (RCB0995). The cells were cultured at 37°C, in a humidified atmosphere containing 5 % CO_2 in MEM supplemented with 10 % heat inactivated fetal bovine serum (FBS), 1 % MNEAA, 1 % Penicillin–Streptomycin. Every 2–3 days, the MDCK cells were detached using 0.25 % trypsin-EDTA solution for passaging.

Characterization of the chemical properties and photoresponsivity of the surface of PAA hydrogels

The chemical properties of the PAA hydrogel substrate surfaces were characterized using cell adhesion tests. We prepared two types of photofunctionalized PAA hydrogel substrates that were fed with cRGD at different concentrations. The concentration of cRGD solutions used for substrate preparation were 50, 400 μM. For the cell adhesion test, MDCK cells were seeded onto the photoactivatable hydrogel surface at 1 × 10^6 cells/dish in MEM which does not contain FBS and cultured in a glass-bottomed dish (φ = 350 mm). This seeding density corresponds to the diameter of the dishes, as described in our previous report [21]. With regards to photoirradiation to the surface, the irradiation (λ = 365 nm) was 10 J/cm^2, where the photocleavage reaction of the 2-nitrobenzyl group is almost completed as reported in our previous report [24]. We washed each substrate with PBS for three times at 2 h after seeding MDCK cells. We then counted the number of cells that adhered to the surface of the hydrogel substrates in the visual field at arbitrary points on the surface of the hydrogel.

Photopatterning and migration induction

To form patterned cellular clusters, we inserted a photomask at the diaphragm slider of the microscope [27]. This system allowed us to choose the area for patterning. The photomask was fabricated by printing the corresponding pattern on a transparency [28]. A piece of the photoactivatable substrate was placed on a glass-bottomed dish (φ = 350 mm) and immersed in PBS. The surface of the photoactivatable substrate was irradiated UV light (λ = 365 nm) with 10 J/cm^2 *via* an

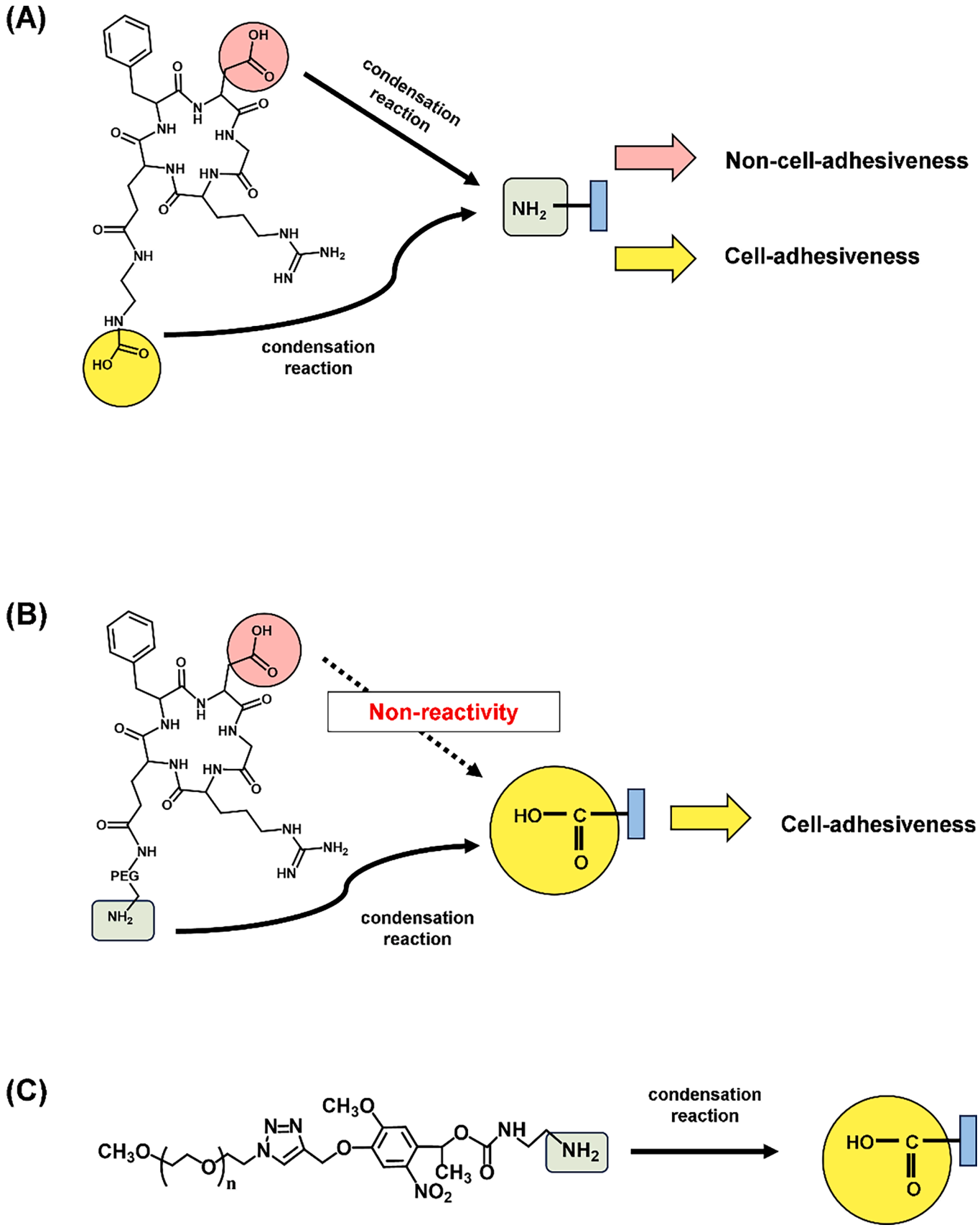

Fig. 2. Cyclic(Arg-Gly-Asp) (cRGD) peptide for chemically defined cell adhesion on the hydrogel surface and new photocleavable poly(ethylene glycol) (PCP) for co-immobilization with cRGD. (A) The problem with immobilizing cRGD on the conventional amino-functionalized hydrogel surface. (B) The new approach for immobilizing cRGD on the material surface. (C) New PCP for reacting surfaces with carboxy groups.

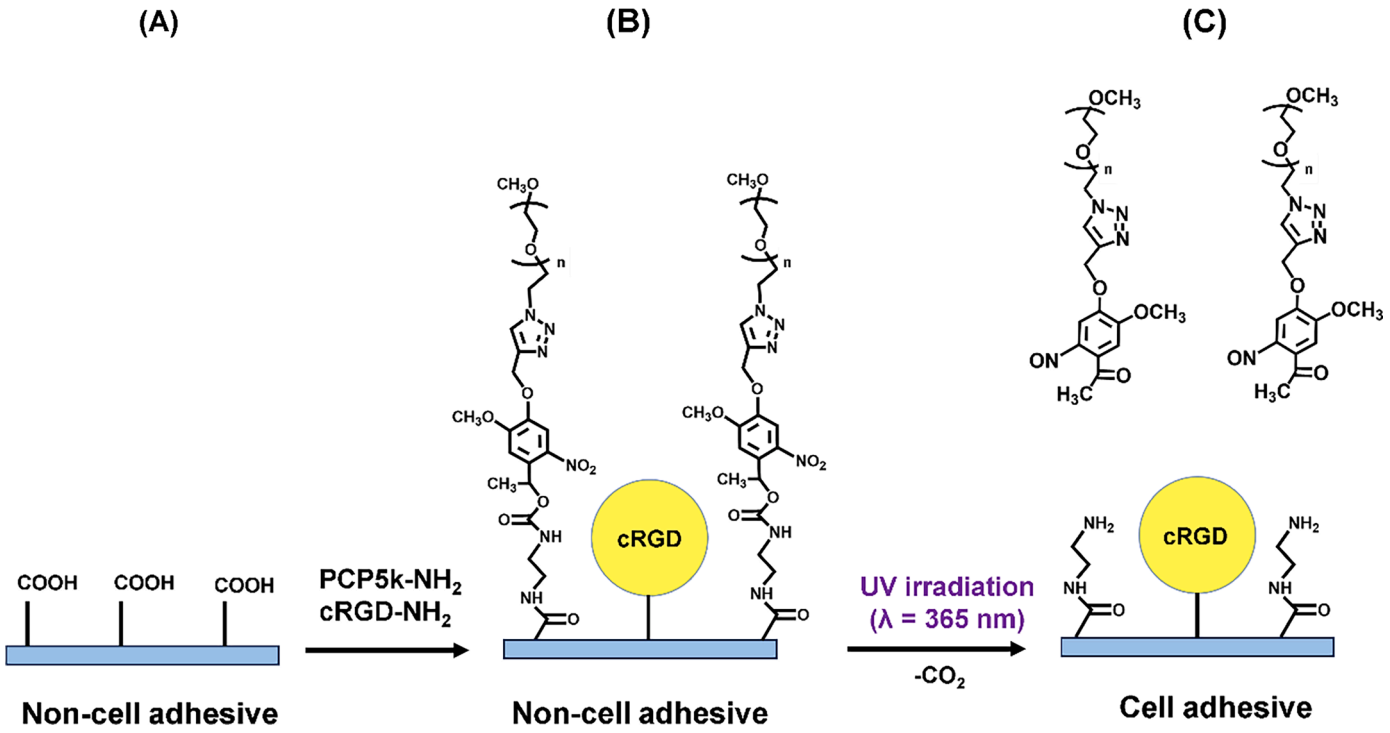

Fig. 3. Schematic representation of the photofunctionalization of the PAA hydrogel surface. PCP5k-NH_2 and cRGD-NH_2 are co-immobilized on the PAA hydrogel surface. This surface becomes cell-adhesive in response to UV light (λ= 365 nm).

appropriate photomask under a fluorescence microscope (IF81-PAFM; Olympus, Tokyo, Japan) or Axiovert 200 (Zeiss, Oberkochen, Germany) equipped with a mercury arc lamp. For each microscope, a cooled CCD camera, Retiga EXi (Qimaging), or Cool SNAP MYO (Photometrics, Tucson, AZ, USA) was used for image capture. All systems were controlled using the Metamorph software (Molecular Devices, Sunnyvale, CA, USA), and the captured images were processed using the ImageJ software (National Institutes of Health, Bethesda, MD, USA). After photoirradiation, MDCK cells were seeded onto the surface at a density of 1×10^6 cells/dish in MEM without FBS. Next, we removed the cells that did not adhere to the surface 2 h after cell seeding by rinsing with PBS. MEM, which did not contain FBS, was then replaced with a medium containing FBS. After medium replacement, the MDCK cells were cultured for 24 h in an incubator. Consequently, collective cellular patterns corresponding to the photopatterns were produced. In addition, collective cell migration was induced by secondary photoirradiation around the cell clusters. Collective cell migration was monitored for 24 h *via* time-lapse imaging with the inverted microscope.

Results and discussion

Design rationale

In this study, PCP and cell-adhesive peptides were co-immobilized on a hydrogel surface to control the chemical and mechanical properties of the material. Generally, either amino- or carboxy-termini are used for peptide conjugation (Fig. 2a). However, when these reactive groups are present in the active center of the peptide, complex protection/deprotection and activation steps are required to conjugate the peptide to the material. cRGD, the most widely known cell-adhesive peptide, has a carboxyl group at its active center. Therefore, we considered it reasonable to conjugate the amino end of the peptide with the hydrogel surface (Fig. 2b). To this end, we synthesized an amino-terminated PCP (PCP5k-NH_2) and reacted it with the activated carboxyl groups of the hydrogel using EDC (Fig. 2c). The new PCP5k-NH_2 and cRGD-NH_2 were co-immobilized on the surface of the PAA hydrogel *via* condensation (Fig. 3). In this state, the PAA surface was non-cell-adhesive because cRGD was under the umbrella of the bulky PEG brushes (Fig. 3a,b). However, irradiation caused the PAA surface to become cell-adhesive as cRGD became available to the cells by photoreleasing PEG (Fig. 3c).

Synthesis of amino-terminated PCP (3)

Amino-terminated PCP with a molecular weight of 5000 (PCP5k-NH_2) (**3**) was synthesized in two steps from the photocleavable heterobifunctional crosslinker molecule (**1**) (Fig. 4). Briefly, a diluted solution of **1** in CH_3CN was added dropwise to excess of 1,2-ethylenediamine (100 equiv.) to minimize dimer formation and yield the desired monomer (**2**) *via* amide coupling with an *N*-hydroxysuccinimide (NHS) ester. Fig. S1 shows ^{1}H NMR spectra of **1** and **2**. In the ^{1}H NMR spectrum of **1**, the resonance signal at 2.79 ppm is coming from the proton on the NHS ester. After the amide coupling, the resonance signal at 2.79 ppm

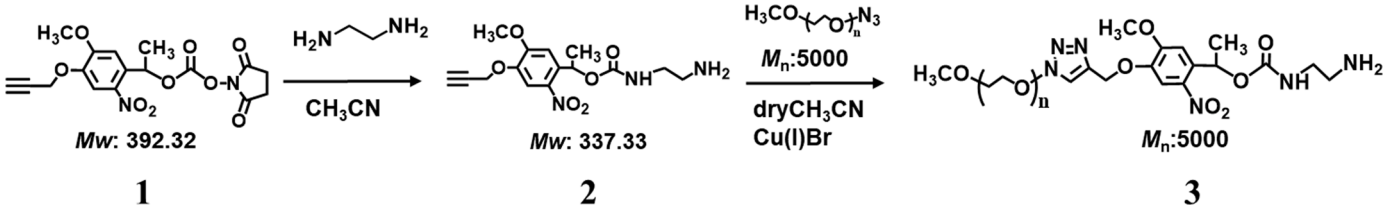

Fig. 4. Synthetic scheme for PCP5k-NH_2 (**3**).

Table 1
Gel indentation assay results for poly(acrylic acid) (PAA) hydrogels.

	(Soft gel)	(Stiff gel)
Expected stiffness [kPa]	5	55
Real stiffness [kPa]	7.5 ± 2.8	52.3 ± 7.4

disappeared, while new resonance signals at 5.21 ppm and 1.30 ppm, which are coming from secondary and primary amine, are observed. This indicated that **2** was successfully synthesized. From this molecule and MeO-PEG5k-N_3, **3** was synthesized *via* copper(I)-catalyzed azide-alkyne Huisgen 1,3-dipolar cycloaddition (click chemistry). **3** was also characterized using ^{1}H NMR spectroscopy. Fig. S2 shows ^{1}H NMR spectra of **2** and **3**. For the ^{1}H NMR spectrum of **2**, the resonance signal at 2.57–2.59 ppm is coming from the alkyne. After the reaction, the resonance signal at 2.57–2.59 ppm disappeared, and new resonance signals at 7.94 ppm were observed from triazole. This indicated that **3** was successfully synthesized.

Preparation of stiffness-tuned photoactivatable PAA hydrogels

Next, as the base material for the photoactivatable cell culture platform, we prepared two different PAA hydrogels with different concentrations of the crosslinker molecule, *N,N'*-methylenebis(acrylamide). A gel indentation assay [26] indicated that the stiffnesses of these two PAA hydrogels were 7.5 ± 2.8 kPa and 52.3 ± 7.4 kPa, and these values agree well with our intended stiffnesses designed based on the previous study (Table 1) [25]. Hereafter, we refer to these two gels as soft and stiff gels, respectively. This result suggests that the stiffness of PAA hydrogels can be tuned by controlling their crosslinking density, and we were able to determine the mechanical properties of the gel substrate. Then, we evaluated the Young's modulus of the hydrogel to determine whether the modification and photodegradation of PCP resulted in unintended values for the stiffness of the hydrogel (Table S1). After PCP was modified on the surface of hydrogels, the hydrogels were slightly softened due to surface swelling, but the stiffness after photo-release of PEG by UV irradiation were not significantly different from that of bare gel (Fig. S3). Therefore, the change in stiffness due to PCP-modification and the photodissociation of PCP will not affect cell behaviors. In addition, cells which adhere on the gel substrate would respond in close to *in vivo* because the stiffness of PAA hydrogels can be tuned close to that of soft tissues (0.1–100 kPa) [29].

Next, the surfaces of the different stiffness PAA hydrogels were functionalized with PCP5k-NH_2 and cRGD-NH_2 by reacting the COOH side groups of PAA with the end amino groups of the two ligands. By changing the mixing ratio of these two ligands, we intended to control the surface cRGD density in cells after the removal of the PEG brushes. However, increasing the fraction of cRGD to make the surface more adhesive is associated with a risk of making the cell surface adhesive even before photoirradiation. Therefore, the optimization of a suitable range of mixing ratios is critical for the development of photoactivatable hydrogels based on this design. We kept the concentration of PCP5k-NH_2 constant and changed the concentration of cRGD to examine its effect on the photoswitchability of the gel surface.

Fig. 5 shows images of MDCK cells allowed to adhere for 2 h on the surface with and without photoirradiation. Depending on the cRGD concentration, the number of adhered cells after photoirradiation was significantly different (Fig. 5a,b). In contrast, cell adhesion was markedly inhibited prior to UV irradiation (Fig. 5a). Cell adhesion could not be completely inhibited; however, the number of cells that unintentionally adhered to the surface was negligible. Therefore, we can produce collective cellular patterns corresponding to photopatterns on the material surface with defined chemical and mechanical properties owing to the photoswitchability of this material.

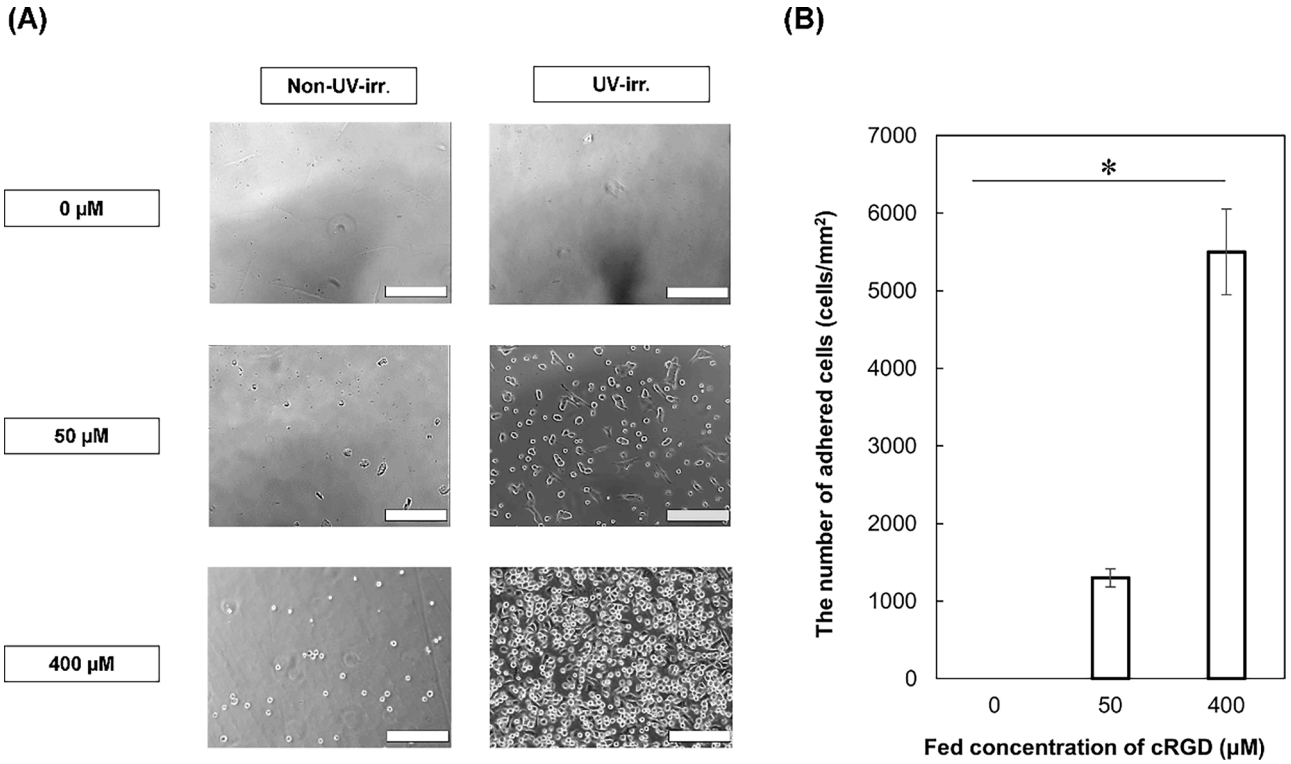

Fig. 5. Cell adhesion test of photoactivatable PAA hydrogels with different cRGD densities. The surface of PAA hydrogels was functionalized with PCP5k-NH_2 (8 mg/mL) and cRGD-NH_2 (0, 50, and 400 μM), and Madin–Darby canine kidney (MDCK) cells were allowed to attach for 2 h. Cells were seeded at 1.0×10^6 cells/dish (φ = 350 mm). (A) Phase-contrast images of MDCK cells on the gel surface with and without photoirradiation. Scale bar, 100 μm. (B) Average number of MDCK cells attached to each surface after photoirradiation. Error bars represent the standard deviation. *Significant difference was analyzed *via* a two-tailed Student's *t*-test ($p < 0.05$; $n = 3$).

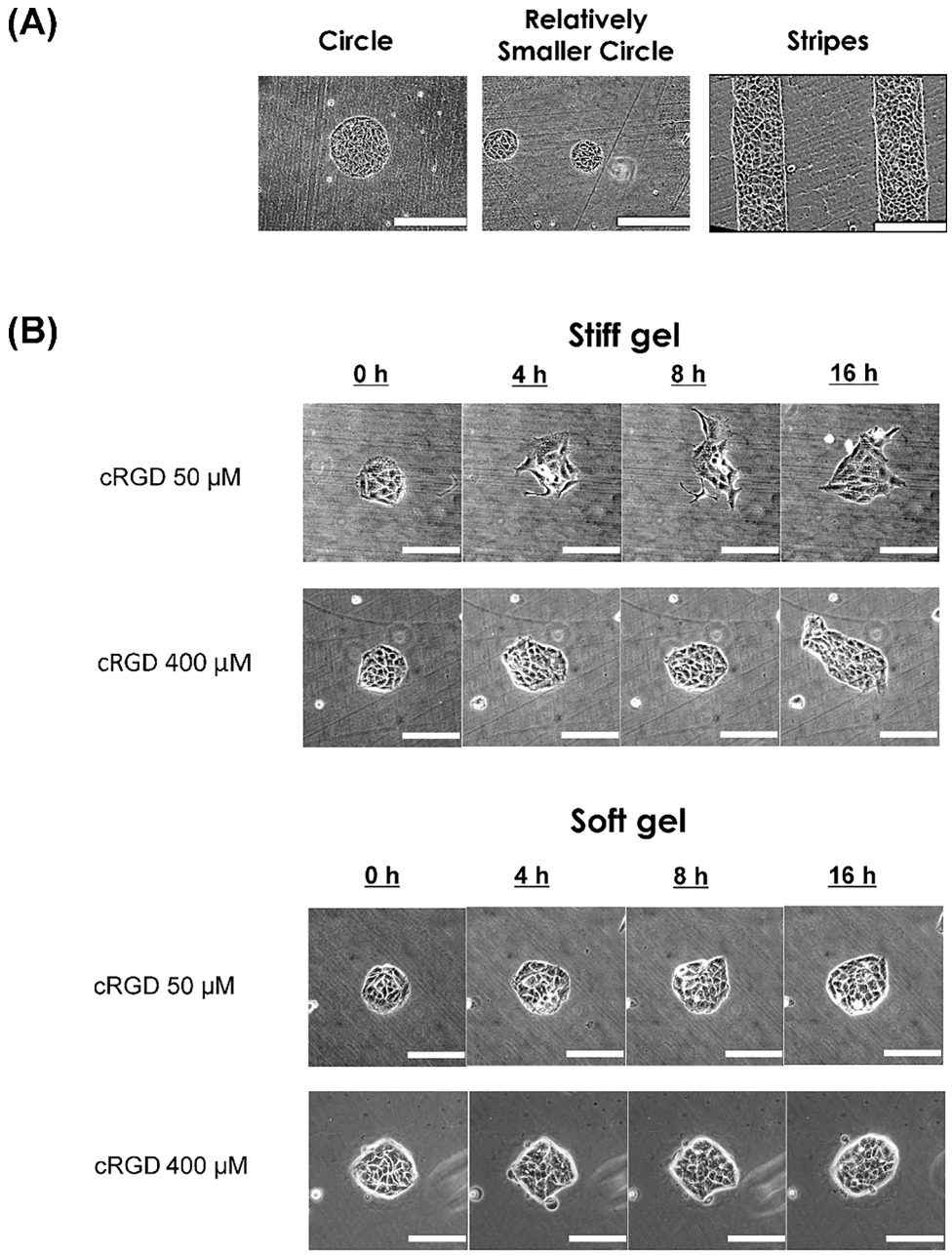

Fig. 6. Spatiotemporal control of cell adhesion to the new photoactivatable substrate. (A) MDCK cells patterned in various geometries on the stiff gel. Scale bar, 100 μm. (B) Phase contrast images of MDCK cells during migration on each photoactivatable substrate after the second irradiation. MDCK cells were confined to a circular spot by the first irradiation, and their migration was induced by the second irradiation of their surroundings. Cells were seeded at 1.0×10^6 cells/dish ($\varphi = 350$ mm). Scale bar, 50 μm.

Photocontrolled cell adhesion and analysis of phototriggered collective cell migration

Next, we used the new photoactivatable substrate for collective cell migration studies. When UV irradiation was applied to the photoactivatable substrate, MDCK cells were confined to the region corresponding to the UV-irradiated region and formed clusters with various geometrical patterns (Fig. 6a). To demonstrate the dynamic photoresponsivity of the substrate, we induced collective cell migration by a second UV irradiation. Collective cell migration was successfully induced using photoirradiation (Fig. 6b). On the other hand, without secondary irradiation, the pattern of the collective cell was retained for 24 h (Fig. S3). Furthermore, the collective cell migration behavior differed according to the elastic modulus and surface density of cRGD on each substrate. Taken together, these results demonstrate that our photoactivatable gel substrates can be used in mechanobiological studies of collective cell migration to explore the interactions between cellular clusters and outside-in signals.

Analysis of the effects of various molecular and mechanical cues on collective cell migration

To further assess the impact of molecular and mechanical cues on collective migration on the developed photoactivatable hydrogels, we investigated the time-dependent changes in the area and circularity of the cell clusters. The former represents the ability of cells to migrate in a manner similar to the cellular travel distance in a wound healing assay. Cluster circularity or roundness represents symmetry breaking of the cell

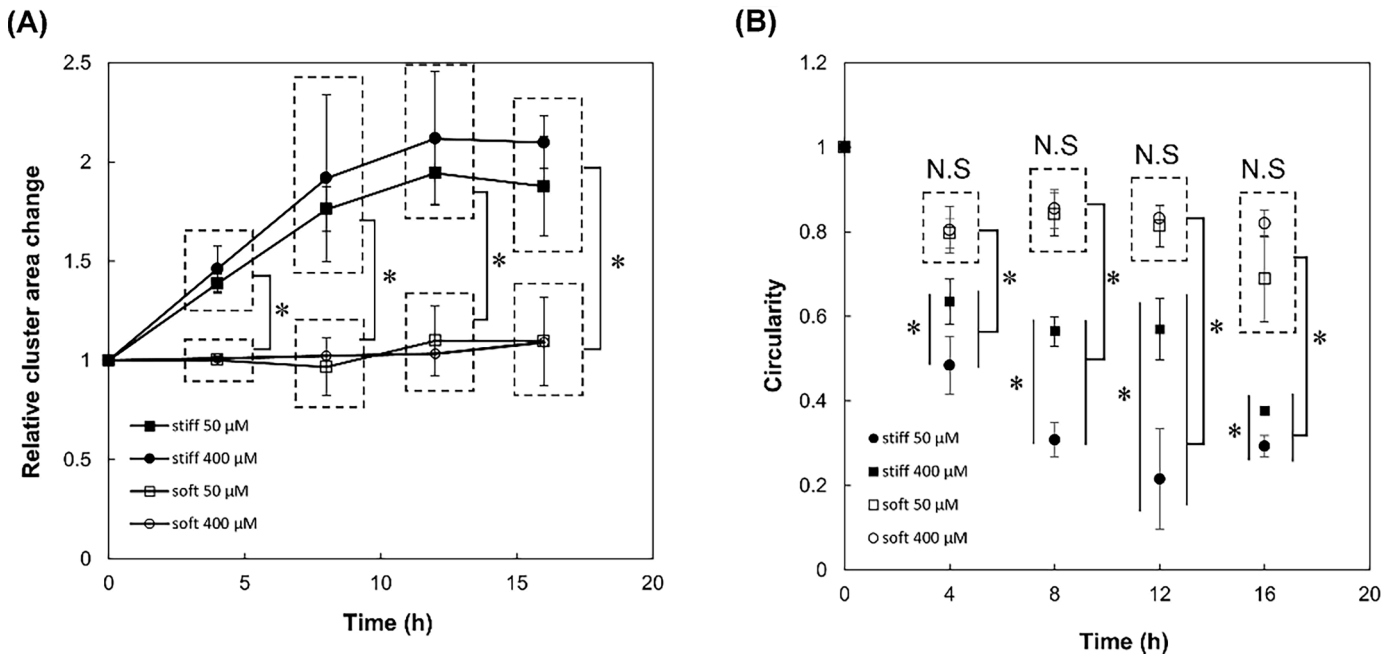

Fig. 7. Characterization of the collective migration behaviors on the photoactivatable gel substrates. (A) Time profiles of cluster area changes on the photoactivatable substrates. (B) Time profiles of the circularity of cellular clusters. Error bars represent the standard deviations. *Significant differences were analyzed *via* a two-tailed Student's *t*-test ($p < 0.05$; $n = 3$).

collectives. Owing to the emergence of leader cells at the cluster boundary, the geometry of the cell clusters differs from the initial circular geometry, which can be detected as a decrease in circularity.

On the stiff gel, the cluster area increased in a time-dependent manner both for high and low cRGD surfaces (Fig. 7A, ■ and ●). In contrast, almost no area increase was observed on the soft gel regardless of the surface cRGD density (Fig. 7a, □ and ○). Significant differences between the stiff and soft gels were observed throughout the observation period. Similar results have been previously reported for collective cell migration [21,23]. From a mechanobiological perspective, this result agrees with the molecular clutch model [30]. These activities may have contributed to the increased cluster expansion on the stiff gels. Fig. 7a also shows that the influence of chemical properties (□ vs. ○ and ■ vs. ●) on cellular cluster area changes is small. Fig. 7b shows the circularity of the cellular clusters during migration. Although the effect of chemical property on the circularity of cellular clusters on the soft gel was negligible (□ vs. ○), its influence on the stiff gel was significant enough to show a clear difference in circularity (■ vs. ●). This result suggests that the symmetry breaking occurs due to the synergistic effect of the chemical and mechanical properties in the elastic range (7.5 ± 2.8 to 52.3 ± 7.4 kPa). Circularity is associated with the formation of leader cells within the cell clusters. Therefore, the marked reduction in the circularity of the low-cRGD surface on the stiff gel indicated enhanced leader-cell formation by synergistically sensing outside-in molecular and mechanical cues from their scaffold.

Conclusions

In summary, we developed a new method for collective cell migration analysis in this study. We synthesized a new photocleavable molecule, PCP5k-NH_2, on which the surface of PAA hydrogels could be functionalized with cell-adhesive peptides. This approach facilitates the control of the cellular cluster geometry on the hydrogel, where the cells are exposed to molecular and mechanical cues. These three cues (geometry, chemistry, and mechanics) can be independently controlled using the same platform. Furthermore, we confirmed the usefulness of our strategy using the cRGD peptide, the most widely used cell-adhesive peptide. By controlling the photoirradiation of this material, we created geometrically defined cellular clusters corresponding to the pattern of photoirradiation and introduction of collective cell migration. Our results provide evidence of the synergetic effects of signals, such as the chemical and mechanical properties, on the collective cell migration behavior. Our approach can be applied to other cell-adhesive peptides, such as YIGSR (Tyr-Ile-Gly-Ser-Arg) and HAVDI (His-Ala-Val-Asp-Ile), to immobilize the material surface along with PCP5k-NH_2. Additionally, this material can be a robust platform to study the crosstalk between the molecular mechanism and mechanical regulations of collective cell migration.

CRediT authorship contribution statement

Kazuhiro Tatematsu: Writing – review & editing, Writing – original draft, Investigation, Formal analysis, Conceptualization. **Shota Yamamoto:** Writing – review & editing, Supervision, Methodology, Investigation, Formal analysis, Conceptualization. **Masao Kamimura:** Writing – review & editing, Supervision, Methodology, Conceptualization. **Kazuo Yamaguchi:** Writing – review & editing, Supervision. **Jun Nakanishi:** Writing – review & editing, Writing – original draft, Supervision, Methodology, Conceptualization.

Declaration of competing interest

The authors declare that they have no known competing financial interests or personal relationships that could have appeared to influence the work reported in this paper.

Data Availability

Data will be made available on request.

Acknowledgements

This study was partially supported by the Japan Society for the

Promotion of Science, Kakenhi (Nos. 22K14705, 22H00596, and 23K17481).

Supplementary materials

Supplementary material associated with this article can be found, in the online version, at doi:10.1016/j.talo.2024.100319.

References

[1] C. Norden, V. Lecaudey, Collective cell migration: general themes and new paradigms, Curr. Opin. Genet. Dev. 57 (2019) 54–60, https://doi.org/10.1016/j.gde.2019.06.013.

[2] P. Friedl, D. Gilmour, Collective cell migration in morphogenesis, regeneration and cancer, Nat. Rev. Mol. Cell Biol. 10 (2009) 445–457, https://doi.org/10.1038/nrm2720.

[3] R. Mayor, S. Etienne-Manneville, The front and rear of collective cell migration, Nat. Rev. Mol. Cell Biol. 17 (2016) 97–109, https://doi.org/10.1038/nrm.2015.14.

[4] K. Doxzen, S.R.K. Vedula, M.C. Leong, H. Hirata, N.S. Gov, A.J. Kabla, B. Ladoux, C.T. Lim, Guidance of collective cell migration by substrate geometry, Integrative Biol. (United Kingdom) 5 (2013) 1026–1035, https://doi.org/10.1039/c3ib40054a.

[5] S. Rausch, T. Das, J.R.D. Soiné, T.W. Hofmann, C.H.J. Boehm, U.S. Schwarz, H. Boehm, J.P. Spatz, Polarizing cytoskeletal tension to induce leader cell formation during collective cell migration, Biointerphases 8 (2013), https://doi.org/10.1186/1559-4106-8-32.

[6] A.E. Miller, P. Hu, T.H. Barker, Feeling Things Out: bidirectional Signaling of the Cell–ECM Interface, Implications in the Mechanobiology of Cell Spreading, Migration, Proliferation, and Differentiation, Adv. Healthc. Mater. 9 (2020) 1–24, https://doi.org/10.1002/adhm.201901445.

[7] A.K. Mishra, J.P. Campanale, J.A. Mondo, D.J. Montell, Cell interactions in collective cell migration, Development (Cambridge) 146 (2019) 1–7, https://doi.org/10.1242/dev.172056.

[8] A.C. Canver, O. Ngo, R.L. Urbano, A.M. Clyne, Endothelial directed collective migration depends on substrate stiffness via localized myosin contractility and cell-matrix interactions, J. Biomech. 49 (2016) 1369–1380, https://doi.org/10.1016/j.jbiomech.2015.12.037.

[9] N. Yamaguchi, T. Mizutani, K. Kawabata, H. Haga, Leader cells regulate collective cell migration via Rac activation in the downstream signaling of integrin β1 and PI3K, Sci. Rep. 5 (2015), https://doi.org/10.1038/srep07656.

[10] K.J. Simpson, L.M. Selfors, J. Bui, A. Reynolds, D. Leake, A. Khvorova, J.S. Brugge, Identification of genes that regulate epithelial cell migration using an siRNA screening approach, Nat. Cell Biol. 10 (2008) 1027–1038, https://doi.org/10.1038/ncb1762.

[11] K.I. Hulkower, R.L. Herber, Cell migration and invasion assays as tools for drug discovery, Pharmaceutics 3 (2011) 107–124, https://doi.org/10.3390/pharmaceutics3010107.

[12] J. Han, N.V. Menon, Y. Kang, S.Y. Tee, An in vitro study on the collective tumor cell migration on nanoroughened poly(dimethylsiloxane) surfaces, J. Mater. Chem. B 3 (2015) 1565–1572, https://doi.org/10.1039/c4tb01783h.

[13] S.Y. Park, H. Jang, S.Y. Kim, D. Kim, Y. Park, S.H. Kee, Expression of e-cadherin in epithelial cancer cells increases cell motility and directionality through the localization of zo-1 during collective cell migration, Bioengineering 8 (2021) 1–17, https://doi.org/10.3390/bioengineering8050065.

[14] S. Nasrollahi, C. Walter, A.J. Loza, G.V. Schimizzi, G.D. Longmore, A. Pathak, Past matrix stiffness primes epithelial cells and regulates their future collective migration through a mechanical memory, Biomaterials 146 (2017) 146–155, https://doi.org/10.1016/j.biomaterials.2017.09.012.

[15] A. Gelmi, C.E. Schutt, Stimuli-responsive biomaterials: scaffolds for stem cell control, Adv. Healthc. Mater. 10 (2021), https://doi.org/10.1002/adhm.202001125.

[16] J. Zhang, C. Cheng, J.L. Cuellar-Camacho, M. Li, Y. Xia, W. Li, R. Haag, Thermally responsive microfibers mediated stem cell fate via reversibly dynamic mechanical stimulation, Adv. Funct. Mater. 28 (2018), https://doi.org/10.1002/adfm.201804773.

[17] J. Nakanishi, S. Yamamoto, Static and photoresponsive dynamic materials to dissect physical regulation of cellular functions, Biomater. Sci. 10 (2022) 6116–6134, https://doi.org/10.1039/d2bm00789d.

[18] S. Kaneko, H. Nakayama, Y. Yoshino, D. Fushimi, K. Yamaguchi, Y. Horiike, J. Nakanishi, Photocontrol of cell adhesion on amino-bearing surfaces by reversible conjugation of poly(ethylene glycol) via a photocleavable linker, Phys. Chem. Chem. Phys. 13 (2011) 4051–4059, https://doi.org/10.1039/c0cp02013c.

[19] S.A. Abdellatef, J. Nakanishi, Photoactivatable substrates for systematic study of the impact of an extracellular matrix ligand on appearance of leader cells in collective cell migration, Biomaterials 169 (2018) 72–84, https://doi.org/10.1016/j.biomaterials.2018.03.045.

[20] Y. Shimizu, M. Kamimura, S. Yamamoto, S.A. Abdellatef, K. Yamaguchi, J. Nakanishi, Facile preparation of photoactivatable surfaces with tuned substrate adhesiveness, Anal. Sci. 32 (2016) 1183–1188, https://doi.org/10.2116/analsci.32.1183.

[21] M. Kamimura, M. Sugawara, S. Yamamoto, K. Yamaguchi, J. Nakanishi, Dynamic control of cell adhesion on a stiffness-tunable substrate for analyzing the mechanobiology of collective cell migration, Biomater. Sci. 4 (2016) 933–937, https://doi.org/10.1039/c6bm00100a.

[22] C.G. Rolli, H. Nakayama, K. Yamaguchi, J.P. Spatz, R. Kemkemer, J. Nakanishi, Switchable adhesive substrates: revealing geometry dependence in collective cell behavior, Biomaterials 33 (2012) 2409–2418, https://doi.org/10.1016/j.biomaterials.2011.12.012.

[23] S. Yamamoto, K. Okada, N. Sasaki, A.C. Chang, K. Yamaguchi, J. Nakanishi, Photoactivatable hydrogel interfaces for resolving the interplay of chemical, mechanical, and geometrical regulation of collective cell migration, Langmuir 35 (2019) 7459–7468, https://doi.org/10.1021/acs.langmuir.8b02371.

[24] J. Nakanishi, Photoactivatable substrates: a material-based approach for dissecting cell migration, Chem. Record 17 (2017) 611–621, https://doi.org/10.1002/tcr.201600090.

[25] R.S. Fischer, K.A. Myers, M.L. Gardel, C.M. Waterman, Stiffness-controlled three-dimensional extracellular matrices for high-resolution imaging of cell behavior, Nat. Protoc. 7 (2012) 2056–2066, https://doi.org/10.1038/nprot.2012.127.

[26] R. Long, M.S. Hall, M. Wu, C.Y. Hui, Effects of gel thickness on microscopic indentation measurements of gel modulus, Biophys. J. 101 (2011) 643–650, https://doi.org/10.1016/j.bpj.2011.06.049.

[27] J. Nakanishi, Y. Kikuchi, T. Takarada, H. Nakayama, K. Yamaguchi, M. Maeda, Photoactivation of a Substrate for Cell Adhesion under Standard Fluorescence Microscopes, J. Am. Chem. Soc. 126 (2004) 16314–16315, https://doi.org/10.1021/ja044684c.

[28] D.C. Duffy, J.C. Mcdonald, O.J.A. Schueller, G.M. Whitesides, Rapid Prototyping of Microfluidic Systems in Poly(dimethylsiloxane), (1998). doi:10.1021/ac980656z.

[29] C.F. Guimarães, L. Gasperini, A.P. Marques, R.L. Reis, The stiffness of living tissues and its implications for tissue engineering, Nat. Rev. Mater. 5 (2020) 351–370, https://doi.org/10.1038/s41578-019-0169-1.

[30] H.E. Balcioglu, L. Balasubramaniam, T.V. Stirbat, B.L. Doss, M.A. Fardin, R. M. Mège, B. Ladoux, A subtle relationship between substrate stiffness and collective migration of cell clusters, Soft. Matter. 16 (2020) 1825–1839, https://doi.org/10.1039/c9sm01893j.